The CD157-Integrin Partnership Controls Transendothelial Migration and Adhesion of Human Monocytes[*]

Nicola Lo Buono[‡1], Rossella Parrotta[‡1,2], Simona Morone[‡3], Paola Bovino[‡], Giulia Nacci[‡], Erika Ortolan[‡§],
Alberto L. Horenstein[‡§], Alona Inzhutova[‡], Enza Ferrero[‡§], and Ada Funaro[‡§4]

From the ‡Laboratory of Immunogenetics, Department of Genetics, Biology and Biochemistry, and §Research Center on Experimental Medicine (CeRMS), University of Torino Medical School, 10126 Torino, Italy

CD157, a member of the CD38 gene family, is an NAD-metabolizing ectoenzyme and a signaling molecule whose role in polarization, migration, and diapedesis of human granulocytes has been documented; however, the molecular events underpinning this role remain to be elucidated. This study focused on the role exerted by CD157 in monocyte migration across the endothelial lining and adhesion to extracellular matrix proteins. The results demonstrated that anti-CD157 antibodies block monocyte transmigration and adhesion to fibronectin and fibrinogen but that CD157 cross-linking is sufficient to overcome the block, suggesting an active signaling role for the molecule. Consistent with this is the observation that CD157 is prevalently located within the detergent-resistant membrane microdomains to which, upon clustering, it promotes the recruitment of β_1 and β_2 integrin, which, in turn, leads to the formation of a multimolecular complex favoring signal transduction. This functional cross-talk with integrins allows CD157 to act as a receptor despite its intrinsic structural inability to do so on its own. Intracellular signals mediated by CD157 rely on the integrin/Src/FAK (focal adhesion kinase) pathway, resulting in increased activity of the MAPK/ERK1/2 and the PI3K/Akt downstream signaling pathways, which are crucial in the control of monocyte transendothelial migration. Collectively, these findings indicate that CD157 acts as a molecular organizer of signaling-competent membrane microdomains and that it forms part of a larger molecular machine ruled by integrins. The CD157-integrin partnership provides optimal adhesion and transmigration of human monocytes.

Ectoenzymes include a heterogeneous group of surface molecules with multiple functions. In addition to interacting with specific substrates, many of them participate in leukocyte activation and migration. In some cases, ectoenzymes exert enzymatic control of leukocyte trafficking (1). Other functions are independent of their enzymatic ability, relying on the activation of signaling cascades that lead to calcium fluxes, cytoskeletal remodeling, and release of inflammatory mediators (2, 3). In selected cases, ectoenzymes associate with adhesion molecules to regulate their signaling (4, 5).

Along with CD38, human CD157 constitutes the NAD glycohydrolase/ADP-ribosyl cyclase gene family (6). These two molecules share 36% of their protein sequence, including 10 cysteine residues forming intrachain disulfide bonds. However, they differ in structure, with CD157 being a glycosylphosphatidylinositol (GPI)[5]-anchored glycoprotein and CD38 being a transmembrane type II glycoprotein (7). CD157 is mainly expressed by cells of the myeloid lineage, bone marrow stroma, and vascular endothelium (8). CD157 is also expressed by ovarian cancer epithelium and by peritoneal mesothelial cells, where it is implicated in tumor dissemination (9). Further, it is endowed with receptor-like features observed in different cell types (10) and transduces signals by interacting with transmembrane partner molecules (11, 12), a strategy shared by other GPI-anchored molecules (13).

CD157 is involved in neutrophil polarization, adhesion, and motility (11) and controls transendothelial migration (14). This study extends the analysis of the functional role of CD157 to human monocytes, adopted as a physiological model in which to explore the molecular mechanism underlying the role of the molecule in the control of cell motility.

Monocytes play key functions in innate and adaptive immunity, immune surveillance, host defense, and inflammation (15). Furthermore, monocyte trafficking is a critical factor in inflammatory and autoimmune diseases, such as atherosclerosis, multiple sclerosis, and rheumatoid arthritis (16).

Monocytes originate from hematopoietic precursors in the bone marrow and circulate in the blood for 24–48 h before extravasating into the connective tissues. In inflammation, monocytes are recruited to the affected tissues, where they differentiate into macrophages and dendritic cells (17). The continuous traffic from blood to tissue and from tissue to lymph nodes relies on orchestrated sequential interactions between leukocytes and vascular or lymphatic endothelium (18). Each

[1] Both authors contributed equally to this work.

[2] Supported by an Italian Association for Cancer Research fellowship.

[3] Supported by a Regione Piemonte fellowship (Ricerca Sanitaria Finalizzata 2009).

[4] To whom correspondence should be addressed: Laboratory of Immunogenetics, Dept. of Genetics, Biology and Biochemistry, University of Torino Medical School, Via Santena 19, 10126 Torino, Italy. Tel.: 39-011-6961734; Fax: 39-011-6966155; E-mail: ada.funaro@unito.it.

[5] The abbreviations used are: GPI, glycosylphosphatidylinositol; F(ab')$_2$ RαMIgG, F(ab')$_2$ fraction of rabbit antibodies to mouse IgG; mIgG, mouse monoclonal IgG; FN, fibronectin; Ctx, cholera toxin β-subunit; MCP-1, monocyte chemoattractant protein-1; HPMEC, human pulmonary microvascular endothelial cell line; ECM, extracellular matrix protein; FAK, focal adhesion kinase; TMI, transmigration index.

step is a prerequisite for the next one. Cell adhesion molecules (such as selectins and integrins) have well established roles in supporting tethering, rolling, and firm adhesion to the vascular endothelium (19). Chemokines and selected molecules at the endothelial junctions (including CD31, JAM-1, vascular endothelial cadherin, and CD99) are critical in the control of the transmigration process (20). These central components are flanked by an increasing number of molecules from different families, which contribute to distinct steps of the extravasation cascade (21).

The results obtained in this study indicate that CD157 is involved in the control of monocyte extravasation and adhesion to ECM proteins. CD157 establishes a structural interaction with β_1 and β_2 integrin and, following antibody-induced cross-linking, it promotes their relocation into detergent-resistant domains, thus driving the dynamic reorganization of signaling-competent membrane microdomains. Moreover, CD157 effectively contributes to the integrin-driven signaling network that is critical during monocyte transmigration.

EXPERIMENTAL PROCEDURES

Antibodies and Reagents—The anti-CD157 (SY/11B5, IgG1), anti-β1 integrin/CD29 (Moon-4, IgG1), anti-CD71 (CB26, IgG2a) mAb, and irrelevant murine monoclonal IgG (mIgG1) were produced in-house. Anti-CD11b (107, IgG1) and anti-β2 integrin/CD18 (TS1/18, IgG1) mAbs were provided by A. Arnaout (Harvard Medical School, Boston, MA). All mAbs were affinity-purified on protein G, and the F(ab')$_2$ fragments were obtained using immobilized papain (Sigma-Aldrich). RF3 (anti-CD157, IgG2a) mAb was from MBL International, D01P (anti-CD157 polyclonal IgG) was from Abnova, 3H1192 (anti-CD29, IgG2a) mAb was from Santa Cruz Biotechnologies, and anti-β actin was from Sigma-Aldrich. Selected mAbs were coupled to Alexa Fluor 488 (Molecular Probes) or Chromis-550 (Cyanagen) according to the manufacturer's instructions. The affinity-purified, F(ab')$_2$ fraction of rabbit antibodies to mouse IgG (F(ab')$_2$ RaMIgG), F(ab')$_2$ RaMIgG labeled with FITC (F(ab')$_2$ RaMIgG-FITC), and streptavidin-Dylight-549 were from Jackson ImmunoResearch Laboratories. Fibronectin (FN), fibrinogen, crystal violet, and FITC or horseradish peroxidase (HRP)-labeled cholera toxin β-subunit (Ctx) were from Sigma-Aldrich. Monocyte chemoattractant protein-1 (MCP-1), TNFα, and IL-1β were from Peprotech.

Cells and Cell Lines—Peripheral blood mononuclear cells were isolated from healthy blood donors by density gradient centrifugation, after informed written consent. Monocyte negative selection was performed via magnetic activated cell sorting using the monocyte isolation kit (Miltenyi Biotec) according to the manufacturer's instructions. This yielded >95% monocytes, as determined by flow cytometry following labeling with anti-CD14-FITC mAb (BD Biosciences).

Human monocytic THP-1 cell line (ATCC, Manassas, VA) was maintained in RPMI 1640 medium supplemented with 5% FCS. The human pulmonary microvascular endothelial cells (HPMEC) were generated as described (22).

Flow Cytometry—Cells (2×10^5/sample) were incubated for 30 min at 4 °C with 5 μg/ml of appropriate primary mAbs, washed, and incubated for 30 min at 4 °C with F(ab')$_2$ RaMIg-

FITC. Fluorescence was determined using a FACSCalibur flow cytometer and analyzed with CellQuest software (BD Biosciences). Background mAb binding was estimated by means of isotype-matched negative control mAb. Ten thousand events were considered for each analysis.

Transendothelial Migration Assay—HPMEC were grown to confluence on 5-μm pore Transwell chambers (Corning-Costar) coated with fibronectin (10 μg/ml) and either left unstimulated or stimulated for 4 h at 37 °C with TNFα (20 ng/ml) or IL-1β (10 units/ml). Peripheral blood mononuclear cells (5×10^5) were treated with the indicated mAbs (10 μg/ml) for 20 min before the assay and then seeded on the HPMEC monolayers. To induce CD157 cross-linking, F(ab')$_2$ RaMIgG (50 μg/ml) was added to the desired samples. After a 2-h incubation at 37 °C, the transmigrated (suspended and adhered) monocytes were collected and counted by FACS at medium speed for 3 min. The transmigration index (TMI) was determined using the formula: TMI = (number of cells migrated in the presence of blocking mAb)/(number of cells migrated in the presence of mIgG).

Cell Adhesion to ECM Proteins—Purified monocytes or THP-1 cells (5×10^4) pretreated with selected mAbs (10 μg/ml for 20 min) were plated onto 96-well plates coated with FN (10 μg/ml) or fibrinogen (50 μg/ml) and blocked with 2% BSA. To induce CD157 cross-linking, F(ab')$_2$ RaMIgG (50 μg/ml) was added to the indicated samples. After a 1-h incubation at 37 °C, non-adherent cells were removed by washing, and adherent cells were fixed with 4% paraformaldehyde and stained with 0.5% crystal violet. Adherent cells were assessed by light microscopy, and five randomly selected fields ($\times10$) for each well were photographed and counted. Each condition was carried out in quadruplicate, and experiments were repeated at least three times.

Isolation of Detergent-insoluble Microdomains (Lipid Rafts) by Sucrose Gradient Centrifugation and Western Blot Analysis—THP-1 cells (5×10^7) were lysed in 0.7 ml of ice-cold MES lysis buffer (25 mM MES, pH 6.5, 5 mM NaF, 1 mM Na$_3$VO$_4$, 2 mM EDTA, 150 mM NaCl, 0.5% Triton X-100, 50 μg/ml aprotinin, and leupeptin). Where indicated, cells were pretreated (10 min at 37 °C) with FN (10 μg/ml), with anti-CD157 mAb (5 μg/ml), or with anti-CD157 mAb followed by F(ab')$_2$ RaMIgG (20 μg/ml for 1 min at 37 °C). Cell lysates were mixed (v/v) with 80% sucrose (w/v in MES buffer), and a step gradient was prepared by overlaying with 30 and 5% sucrose/MES. After centrifugation at 200,000 $\times$ g for 16 h at 4 °C, 12 fractions (0.4 ml/each) were collected starting from the top of the gradient. Equal amounts of each fraction were resolved on 10% SDS-PAGE under non-reducing conditions, transferred to polyvinylidene difluoride (PVDF) membranes, and subjected to Western blotting with the indicated mAbs followed by RaMIgG-HRP and then developed using an ECL-based system (PerkinElmer Life Sciences). The lipid raft marker GM1 was detected by dot blot analysis using HRP-labeled Ctx.

Immunofluorescence and Confocal Microscopy—Serum-starved cells were fixed in Hanks' balanced salt solution (pH 6.5) containing 2% paraformaldehyde and 1 mM ZnCl$_2$ for 20 min, washed twice in Hanks' balanced salt solution, and treated for 30 min with 50 mM glycine in Hanks' balanced salt solution

supplemented with 1% FCS to quench the aldehyde groups (23). Fixed cells were double-stained with anti-CD157-Chromis-550 and anti-CD18- or CD29-Alexa Fluor 488 mAbs or Ctx-FITC. In selected experiments, cells were incubated with anti-CD157-biotin (5 μg/ml for 10 min on ice), washed, and reacted with streptavidin-Dylight-549 (20 μg/ml for 10 min on ice) and then placed at 37 °C for 2 min to induce capping, blocked by ice-cold PBS with 0.5% BSA and 0.1% NaN$_3$, and fixed as above. Counterstaining was performed with anti-CD18-, CD29-, or CD71-Alexa Fluor 488 mAbs or Ctx-FITC. Engagement of integrins was induced by incubating THP-1 cells (5×10^6/ml) in Hanks' balanced salt solution with FN (10 μg/ml) at 37 °C for 10 min. Cells were fixed, stained with the indicated mAbs, and analyzed by confocal microscopy, using an Olympus FV300 laser scanning confocal microscope equipped with two helium neon (543 and 582 nm) lasers, a blue argon (488 nm) laser, and FluoView 300 software (Olympus Biosystems). Cells were imaged using a $\times$60 oil immersion objective (1.4 NA). Images of optical sections (512×512 pixels) were digitally recorded and processed using Adobe Photoshop CS4 (Mountain View, CA) software. For co-localization analysis, all image data were preprocessed prior to quantification by means of an iterative constrained Tikhonov-Miller algorithm (DeconvolutionLab ImageJ plugin (24)) to reduce the blurring from nearby bright objects and the out-of-focus noise. Co-localization was evaluated using the Colocalization Colormap script, an ImageJ plugin for automated quantification and visualization of co-localized fluorescent signals (25). The method computes correlation of intensities between pairs of individual pixels in two different channels. Results are presented as mean correlation index (I_{corr})$\pm$ S.E. I_{corr} indicates the fraction of positively correlated pixels in the image.

Co-immunoprecipitation Assays—THP-1 cells were treated with 0.5 mM membrane-impermeable cross-linker dithiobis sulfosuccinimidylpropionate (Pierce) for 30 min at 20 °C. The reaction was stopped with 20 mM Tris for 15 min, and then cells were washed and lysed in ice-cold MES buffer. Cell lysates were centrifuged at $14,000 \times g$ for 30 min, precleared overnight with protein G-Sepharose beads, and then incubated overnight at 4 °C with protein G-Sepharose beads conjugated to 2 μg of anti-CD157, anti-CD18, anti-CD29, or anti-CD71 mAbs. The beads were washed with PBS, and proteins were eluted by adding non-reducing Laemmli sample buffer and boiling for 5 min. Eluted proteins were resolved on 10% SDS-PAGE under non-reducing conditions, transferred to PVDF membranes, and probed with mAbs to CD157, CD18, CD29, or CD71 followed by HRP-conjugated secondary antibodies and then detected using ECL.

Phosphorylation Assay—THP-1 cells (2×10^7/ml) were incubated with anti-CD157, anti-CD18, and anti-CD29 mAb (5 μg/ml) for 10 min at 4 °C, washed in cold PBS, cross-linked with F(ab')$_2$ RαMIgG (20 μg/ml), and incubated at 37 °C for 1 min. Cells were placed on ice, washed in cold PBS supplemented with 1 mM Na$_3$VO$_4$ to stop the reaction, and lysed in ice-cold radioimmune precipitation buffer (50 mM Tris HCl, 150 mM NaCl, 1% Nonidet P-40, 0.5% sodium deoxycholate, 1 mM EDTA, 0.1% SDS supplemented with 1 mM Na$_3$VO$_4$, 5 mM NaF, 50 μg/ml aprotinin and leupeptin). After centrifugation, total

lysates (30 μg/lane) were run on 10% SDS-PAGE under reducing conditions and transferred to PVDF membranes. Membranes were blocked and probed with HRP-labeled anti-phosphotyrosine (PY20) polyclonal antibody, anti-phospho-ERK1/2 (Tyr-204/Tyr-187) (BD Biosciences), anti-phospho-c-Src (Tyr-530), anti-phospho-FAK (Tyr-397), and anti-phospho-AKT (Ser-493) (Santa Cruz Biotechnologies). The membranes were stripped and reprobed with anti-ERK2, anti-c-Src, anti-FAK, and anti-AKT1 mAb (Santa Cruz Biotechnologies) followed by incubation with the appropriate HRP-conjugated antibodies. Specific bands were visualized by ECL.

Statistical Analysis—Unless otherwise indicated, values are expressed as means $\pm$ S.E. Comparisons between two groups were carried out using the Student's t test for normal distributed variables. One-way analysis of variance with Bonferroni post test correction was used for multiple comparisons. Statistical analyses were performed using Prism 5, GraphPad software (San Diego, CA). Differences were considered statistically significant for p values $\leq$0.05.

RESULTS

CD157 Expression on Circulating Monocytes Is Up-regulated by MCP-1—Flow cytometric analysis confirmed that CD157 is expressed by virtually all the circulating monocytes (Fig. 1A) and demonstrated that its expression rapidly increases upon activation with MCP-1, reaching a plateau after 30 min of stimulation (Fig. 1, A and B). As expected, CD11b expression was enhanced by MCP-1 (Fig. 1B) (26). Immunoblot further proved that CD157 is expressed by monocytes (data not shown) as well as the human monocytic THP-1 cells at the expected molecular weight (see below, Fig. 5A). Up-regulation of monocytic CD157 expression by MCP-1, a chemoattractant factor that promotes monocyte migration and diapedesis, suggested the potential involvement of CD157 in monocyte trafficking.

CD157 Is Involved in Monocyte Transendothelial Migration—A central aspect of leukocyte trafficking is the continuous transition from the blood circulation into the tissues and back. The vascular endothelium constitutes the interface between the two tissue compartments, so transendothelial migration represents a critical step of leukocyte trafficking.

The potential role of CD157 in regulating transmigration was explored in a conventional *in vitro* assay using primary monocytes treated with a blocking anti-CD157 mAb or with an anti-CD31 mAb used as a positive control for blocking transmigration (27). To avoid interfering with the Fc receptors expressed by monocytes, F(ab')$_2$ mAbs were used. Because the majority of leukocyte traffic occurs *in vivo* primarily through the microvessels, we used HPMEC as monolayers to reproduce a more physiological environment. These experiments were initially done with resting HPMEC monolayers across which monocytes migrate in response to basal concentrations of chemoattractants, such as MCP-1 (28). The results demonstrated that CD157 ligation by a specific mAb resulted in significant inhibition of transmigration of monocytes, comparable with that obtained with a blocking mAb to CD31. Anti-CD157-mediated inhibition was dose-dependent with significant effects down to 0.4 μg/ml (Fig. 1C).
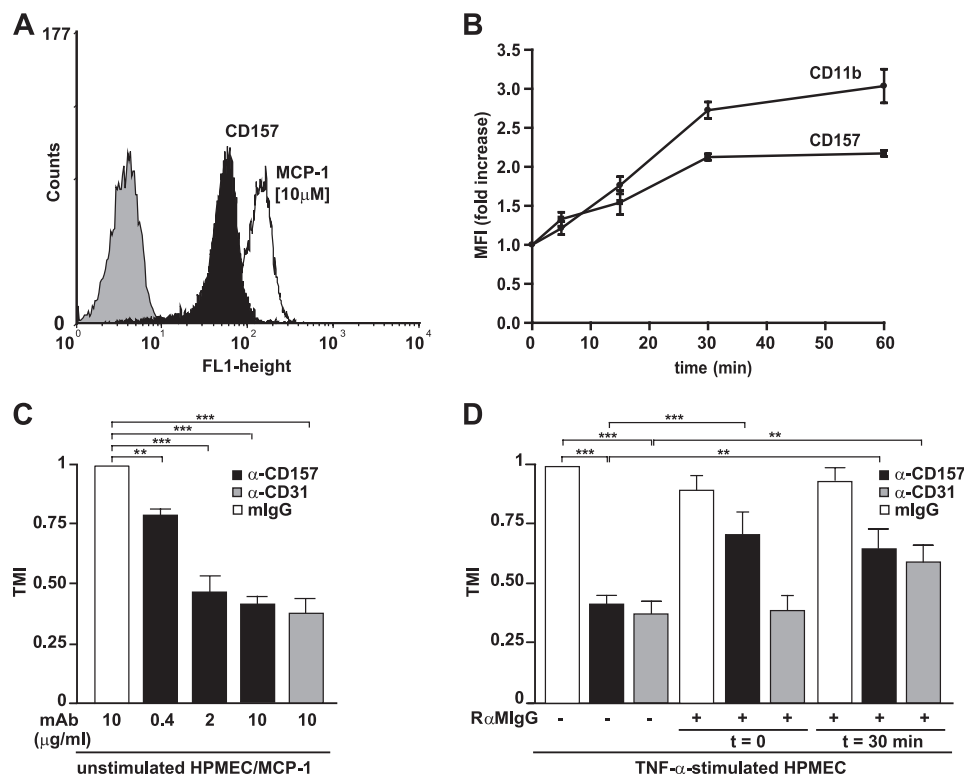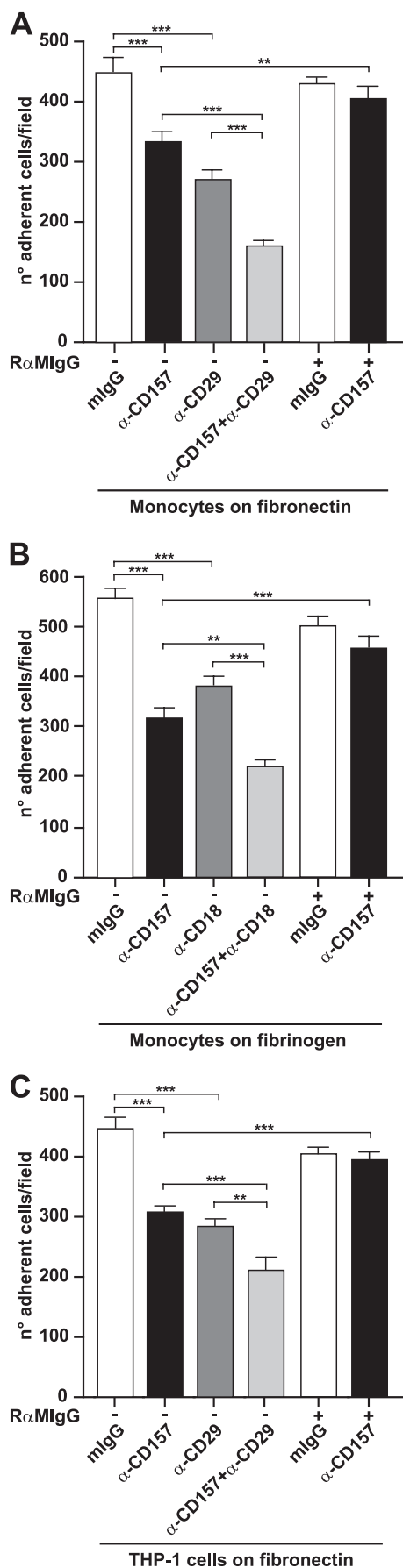
FIGURE 1. **CD157 is expressed in human monocytes and is involved in transendothelial migration.** *A*, representative flow cytometric analysis of surface expression of CD157 on monocytes (*black peak*) or on monocytes stimulated with MCP-1 for 30 min (*white peak*). The *gray peak* indicates the isotype-matched control mAb. Ten thousand events were considered for each analysis. The results presented are representative of three experiments. *x* axis = fluorescence intensity (*FL-1-height*), and *y* axis = number of cells (events). *B*, monocytes were treated with 10 μM MCP-1 for the indicated time at 37 °C, fixed, and incubated with anti-CD157 or anti-CD11b mAb followed by F(ab')$_2$ RαMIgG-FITC. Results showing the increasing rate of mean fluorescence intensity (*MFI*) are expressed as MCP-1-induced expression of CD157/basal or of CD11b/basal surface expression of each molecule at 37 °C. The results are expressed as means of three separate experiments $\pm$ S.E. *C*, transmigration assays across resting HPMEC grown on fibronectin-coated Transwell filters were performed toward a 10 μM MCP-1 Transwell gradient in the presence of increasing concentrations of F(ab')$_2$ anti-CD157 (*black bars*), anti-CD31 mAb (*gray bar*), or mIgG (*white bar*) (10 μg/ml). After a 2-h incubation at 37 °C, the number of transmigrated monocytes was assessed by FACS at medium speed for 3 min. Results are the mean $\pm$ S.E. of three separate experiments and are expressed as TMI. Anti-CD157 blocked transmigration in a dose-dependent manner. **, $p < 0.01$ and ***, $p < 0.001$. *D*, cross-linking monocyte CD157 reverses the anti-CD157-induced block in transmigration. Monocytes pretreated with F(ab')$_2$ anti-CD157 (*black bars*), anti-CD31 mAb (*gray bars*), or mIgG (*white bars*) (10 μg/ml) were added to HPMEC monolayers activated with TNF-α (20 ng/ml) for 2 h at 37 °C. Where indicated, CD157 and CD31 were cross-linked (at time 0 or 30 min after the beginning of the transmigration) by the addition of a F(ab')$_2$ RαMIgG (50 μg/ml). After a 2-h incubation at 37 °C, transmigrated monocytes were counted as above. Results are expressed as TMI and are the mean $\pm$ S.D. of three replicates. One representative experiment of five is shown. **, $p < 0.01$ and ***, $p < 0.001$.

In concert with neutrophils, monocytes and tissue macrophages participate in inflammatory responses. Therefore, the role of CD157 in transendothelial migration was investigated using cytokine-activated HPMEC monolayers, thereby simulating an inflammatory microenvironment. Stimulation with TNFα or IL-1β had no effect on the surface expression or distribution of CD157 on endothelial cells (14). Ligation of CD157 with a specific mAb significantly reduced transmigration across TNFα-activated HPMEC (Fig. 1*D*) or across IL-1β-activated HPMEC (data not shown). To mimic the extent of CD157 clustering likely occurring on monocytes during transmigration, monocytes were treated with anti-CD157 mAb, and then cross-linking of CD157 was induced by the addition of F(ab')$_2$ RαMIgG prior to their addition to the HPMEC monolayer ($t = 0$). Alternatively, monocytes treated with anti-CD157 mAb were seeded on HPMEC monolayers for 30 min (a sufficient time for monocytes to get to endothelial junctions), and then CD157 cross-linking was performed. Antibody-induced clustering of CD157 overcame the block and significantly restored monocyte transmigration. The effect was independent of the timing of cross-linking (Fig. 1*D*). Antibody-induced cross-link-

ing of CD31 at the start of the assay ($t = 0$) failed to reverse the blockade, whereas it was effective when performed at $t = 30$ min (Fig. 1*D*), as described (29). These data gave raise to the hypothesis that clustering of CD157 might function as a switch that controls transmigration by eliciting intracellular signaling.

CD157 Controls Monocyte Adhesion to Extracellular Matrix Proteins—Adhesion of leukocytes to the extracellular matrix is essential for migration across blood vessels and subsequently into the stroma of inflamed tissues (30). It is regulated by a wide variety of cell surface receptor systems, the most relevant of which belong to the β_1 and β_2 integrin subfamilies.

The contribution of CD157 in regulating the adhesion of monocytes to fibronectin and fibrinogen (*i.e.* the elective extracellular ligands of β_1 and β_2 integrin, respectively) was assessed by performing *in vitro* experiments using monocytes or THP-1 cells treated with anti-CD157 mAbs. Ligation of CD157 significantly reduced the ability of monocytes (Fig. 2, *A* and *B*) and THP-1 cells (Fig. 2*C*) to adhere to both ECM proteins. As expected, cell binding to fibrinogen and fibronectin was inhibited by neutralizing antibodies to CD29 (β_1 integrin) (Fig. 2, *A* and *C*) and CD18 (β_2 integrin)(Fig. 2*B*), respectively. Combined

FIGURE 2. **Effect of CD157 on the adhesion of monocytes to fibrinogen and fibronectin.** *A–C*, monocytes (*A* and *B*) or THP-1 cells (*C*) were treated with the indicated mAbs (10 μg/ml for 20 min). CD157 cross-linking was induced by the addition of F(ab')$_2$ RαMIgG (50 μg/ml for 20 min) where indicated. Cells were plated onto 96-well plates coated with FN or fibrinogen and incubated for 1 h at 37 °C, and then washed, fixed, and stained with crystal violet. The number of monocytes that had adhered to ECM proteins was counted in five randomly selected fields in each well. Results represent the mean ± S.E. of three experiments performed in quadruplicate. **, $p < 0.01$ and ***, $p < 0.001$.

ligation of CD157 and CD29 or CD157 and CD18 resulted in an increased inhibition on both monocyte and THP-1 cell adhesion. However, none of the experimental conditions analyzed entirely abrogated cell adhesion, indicating that other molecules must also participate. Strikingly, CD157 clustering induced by cross-linking with a secondary antibody reversed the blockade and virtually completely restored monocyte (Fig. 3, *A* and *B*) and THP-1 cell (Fig. 3*C*) adhesion. Taken together, these data suggested the existence of a functional interplay between CD157 and both β_1 and β_2 integrin orchestrating critical steps of leukocyte trafficking and corroborate the hypothesis that CD157 is involved in intracellular signal transduction.

CD157 Engagement Recruits β_1 and β_2 Integrins to Detergent-resistant (Lipid Raft) Domains—Next, the possibility that CD157 was engaged in the transduction of activation signals regulating monocyte functions was investigated. The GPI-mediated anchorage to the membrane, indicating the lack of a transmembrane domain of CD157, fostered the hypothesis that it could fulfill receptor functions in the context of membrane microdomains, as part of multimolecular complexes. To address this issue, THP-1 cells (used as a monocyte model) were subjected to lysis and discontinuous sucrose gradient centrifugation to separate detergent-resistant (lipid rafts) from detergent-sensitive (non-rafts) membrane fractions. To validate the fractionation procedure, Ctx was used to identify ganglioside GM1, a major constituent of lipid rafts, whereas CD71 (a raft-excluded protein) was chosen as a marker of the detergent-sensitive fractions. In standard culture conditions and like many other GPI-anchored molecules (31), CD157 almost exclusively associated to detergent-insoluble fractions. A substantial portion of both β_1 (CD29) and β_2 (CD18) integrins was found outside the detergent-insoluble fractions (Fig. 3*A*). When THP-1 cells were treated with anti-CD157 mAb, which can cross-link two CD157 molecules, the membrane compartmentalization of CD157, CD18, and CD29 was similar to that observed in untreated cells (Fig. 3*B*). To exclude that the observed membrane compartmentalization of CD157 and integrins represented an artifact of detergent extraction, confocal microscopy analysis was performed in parallel on live THP-1 cells. This approach showed that CD157 had a characteristic patched pattern in basal conditions and largely co-localized with GM1 gangliosides. In contrast, CD18 and CD29 were uniformly localized on the cell membrane (Fig. 4, *A* and *D*, *left*, and *E*).

To establish whether cross-linking of many CD157 molecules accompanied the reorganization of the membrane topology, the distribution of CD157, CD18, and CD29 molecules on the cell membrane was monitored after CD157 clustering, using biochemical approaches and confocal microscopy.

FIGURE 3. **CD157 engagement recruits β_1 and β_2 integrins to lipid rafts.** *A–D*, THP-1 cells untreated (*A*), treated with F(ab')$_2$ anti-CD157 mAb (5 μg/ml) (*B*), treated with F(ab')$_2$ anti-CD157 mAb (5 μg/ml) followed by F(ab')$_2$ RαMIgG (20 μg/ml for 1 min at 37 °C) (*C*) or treated with fibronectin (10 μg/ml for 10 min at 37 °C) to induce cross-linking (*D*) were lysed in cold MES buffer and fractionated on a sucrose gradient as described under "Experimental Procedures." Aliquots of the 12 recovered fractions were resolved on 10% SDS-PAGE and immunoblotted with mAb to CD157, CD18, and CD29 followed by RαMIgG-HRP. Localization of the GM1 ganglioside (detected by Ctx-HRP) and of CD71 was checked by dot blot analysis as a control of the proper separation of the detergent-resistant (rafts 3–7) and detergent-sensitive (non-rafts 8–12) fractions, respectively. One representative experiment of four is shown. *WB*, Western blot.

CD157 cross-linking by means of a mAb followed by the addition of a secondary antibody triggered the recruitment into the raft fractions of significant amounts of CD18 and CD29 (Fig. 3*C*). Confocal microscopy analysis on live cells confirmed these results. CD157 molecules were induced to cap by mAb cross-linking at 37 °C, and the membrane fluidity and energy intake (required to induce clustering of molecules) were blocked by incubation of the cells on ice in the presence of NaN$_3$ and successive fixation. Upon primary and secondary antibody binding, CD157 molecules and the area of the cell membrane with the highest concentration of GM1 gangliosides localized at the same pole of the cell membrane (Fig. 4*B*, *bottom*). Co-capping experiments highlighted that polar aggregation of CD157 induced CD18 and CD29 to localize in identical areas of the membrane in the majority of cells (Fig. 4, *B* and *D*, *middle*, and *E*). These results indicated that CD157 clustering in human monocytes led β_1 and β_2 integrins into the rafts.

Increasing evidence suggests that ligand-induced oligomerization causes the activation of integrins and provides the stimulus for their association with rafts (32, 33). It was reasonable to expect that ligand-induced integrin oligomerization would cause their lateral association with CD157. To test this hypothesis, clustering of integrins was induced by incubating THP-1 cells with fibronectin. As anticipated, integrin engagement by fibronectin shifted a significant fraction of both CD18 and CD29 from the non-raft to the raft compartment (Fig. 3*D*). Next, the effects of interaction with fibronectin on integrin compartmentalization into lipid rafts were examined by confocal microscopy. Capping of CD29 and CD18 induced by THP-1 incubation with fibronectin was accompanied by co-localization with CD157 (Fig. 4, *C* and *D*, *right*) in 84 and 74% of the

cells, respectively (Fig. 4*E*). No co-localization of CD157 with CD71 was observed in any of the experimental conditions adopted (Fig. 4, *D* and *E*). Together, these results confirmed that CD157 and integrins are interdependent partners in a functional biological network.

CD157 Is Physically Associated with β_1 and β_2 Integrins on Monocyte Membrane—The observation that cross-linking of CD157 induced co-localization of β_1 and β_2 integrins in the same areas on the membrane of THP-1 cells suggested that they might be physically associated. To test this hypothesis, we performed co-immunoprecipitation experiments. The results showed that the anti-CD157 mAb recognized its 45-kDa target protein in the anti-CD18 as well as in the anti-CD29 eluates. Reciprocally, anti-CD29 and anti-CD18 mAb were able to react with the expected 130- and 95-kDa bands, respectively, in the anti-CD157 mAb eluates. However, the anti-CD71 mAb failed to recognize its target protein in any of the eluates; reciprocally, anti-CD157, anti-CD18, and anti-CD29 mAbs failed to react with their target proteins in the anti-CD71 eluates, demonstrating specificity (Fig. 5*A*). These results indicated that, as we demonstrated in granulocytes (12), CD157 is likewise physically bound to both β_1 and β_2 integrin at the cell surface of human monocytes. These observations strongly support the hypothesis of functional cross-talk between CD157 and integrins instrumental to the control of monocyte transmigration.

CD157 Exerts Receptor Activities in Human Myeloid Cells— Topographic relocation of activated receptors, including integrins, into lipid rafts provides foci of intracellular signaling for the cell and may be considered a general mechanism that guarantees leukocyte functions. Therefore, molecules (such as CD157) that promote raft association are likely to effectively
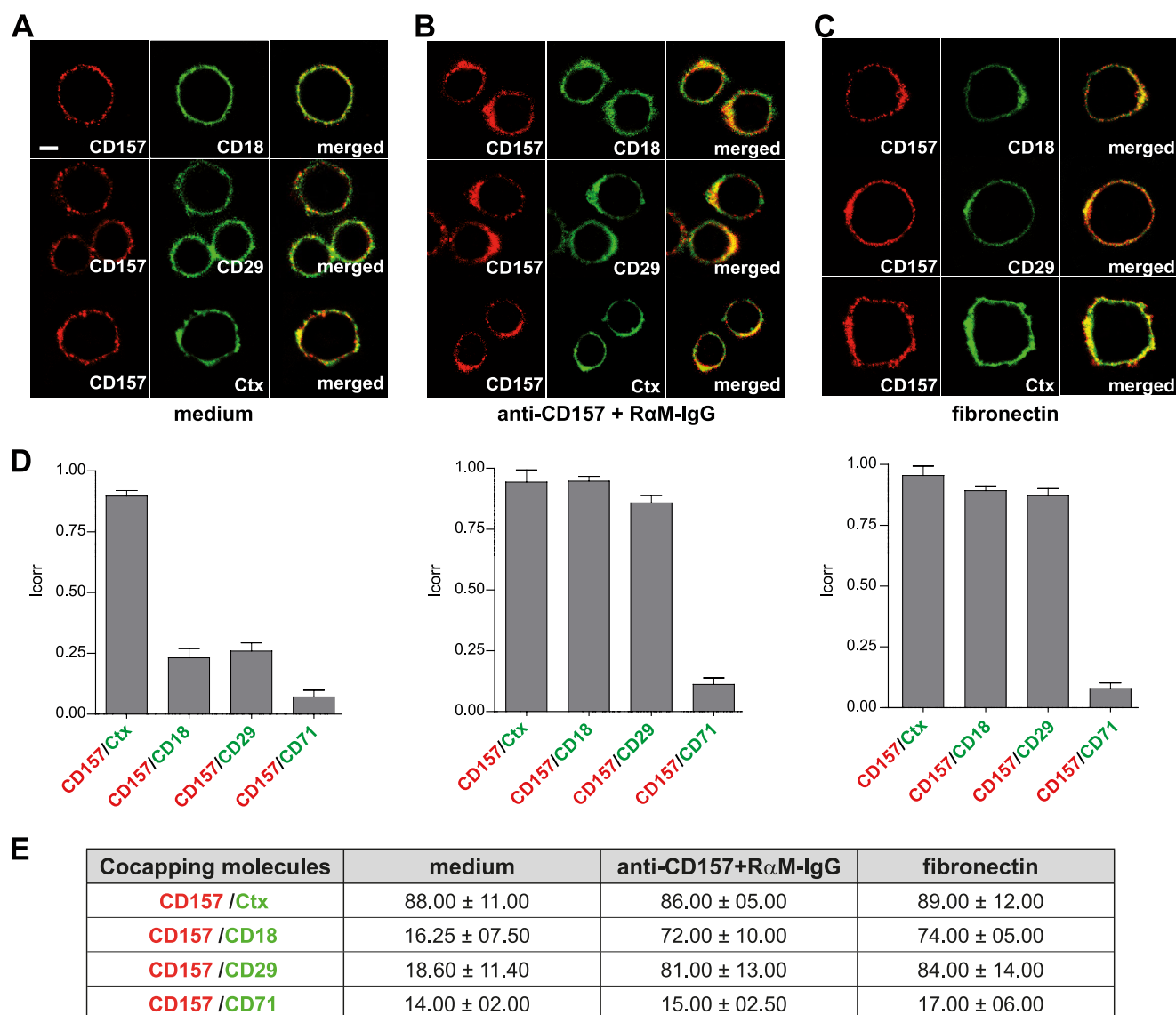
Cocapping molecules	medium	anti-CD157+RαM-IgG	fibronectin
CD157 /Ctx	88.00 ± 11.00	86.00 ± 05.00	89.00 ± 12.00
CD157 /CD18	16.25 ± 07.50	72.00 ± 10.00	74.00 ± 05.00
CD157 /CD29	18.60 ± 11.40	81.00 ± 13.00	84.00 ± 14.00
CD157 /CD71	14.00 ± 02.00	15.00 ± 02.50	17.00 ± 06.00

FIGURE 4. **Confocal microscopy and quantitative analysis of co-localization of CD157 and CD18 or CD157 and CD29 in live cells.** *A*, THP-1 cells were stained with anti-CD157-Chromis-550 (*red*), fixed, and stained with anti-CD18-Alexa Fluor 488 (*green*) or anti-CD29-Alexa Fluor 488 mAbs or Ctx-FITC. *B*, THP-1 cells were stained with anti-CD157-biotin mAb followed by streptavidin-Dylight-549 (*red*) at 4 °C and then moved to 37 °C for 2 min to induce capping. After fixation, cells were stained with anti-CD18-Alexa Fluor 488 or anti-CD29-Alexa Fluor 488 mAbs or Ctx-FITC. *C*, THP-1 cells were treated with fibronectin (10 μg/ml for 10 min at 37 °C) and then fixed and stained with anti-CD157-Chromis-550 and anti-CD18-Alexa Fluor 488 or anti-CD29-Alexa Fluor 488 mAbs or Ctx-FITC. Cells were mounted onto slides and imaged using a confocal scanning laser microscope (FV300) mounted on an IX71 inverted microscope (Olympus, Hamburg, Germany) with a PlanApo ×60 oil immersion objective, 1.4 numerical aperture (NA) objective lens. Images are from a single focal plain scan of the Z stacks. The results of one representative experiment of three are shown. *Scale bar*: 10 μm. *D*, co-localization of CD157 and Ctx, CD157 and CD18, CD157 and CD29, or CD157 and CD71 in THP-1 cells unstimulated (*left*), activated by CD157 cross-link (*middle*), or activated by FN (*right*) was quantified in 60–80 cells in each sample using the Colocalization Colormap script ImageJ plugin for automated quantification and visualization of co-localized fluorescent signals. Histograms represent the mean correlation index (I$_{corr}$)± S.E. of Chromis-550/Alexa Fluor 488 (or FITC) or Dylight-549/Alexa Fluor 488. *E*, the percentage ± S.D. of THP-1 cells showing co-localization of the indicated molecules in the indicated experimental conditions.

contribute to the transduction of intracellular signals that trigger the effector functions.

Further insights into signaling events driven by CD157 in monocytic cells were gathered by exploring the phosphorylation pathway induced on THP-1 cells through antibody-mediated cross-linking. Experiments were performed in parallel using anti-CD18 and anti-CD29 mAbs. Western blot analysis of the proteins tyrosine phosphorylated after short term stimulation at 37 °C demonstrated that CD157 clustering induced a rapid and transient increase of phosphorylation of a broad range of molecules, largely shared with the target substrates of

CD18- and/or CD29-mediated activation pathways (Fig. 5*B*). The increase in phosphorylation reached a peak at 1 min and persisted for ~5 min, declining thereafter (data not shown). The most relevant bands featuring increased intensity as compared with the basal condition (*i.e.* cells treated with F(ab')$_2$ RαMIgG for 1 min at 37 °C) were at 130, 110, 65, 44, and 42 kDa (as indicated by *arrows*) (Fig. 5*B*). Western blot analysis performed using substrate-specific antibodies indicated that target substrates included FAK (p130), c-Src (p65), the serine/threonine kinase Akt (a key downstream effector of p110 phosphoinositide 3-kinase), and MAPK ERK1/2 (p42–44) (Fig. 5*C*).
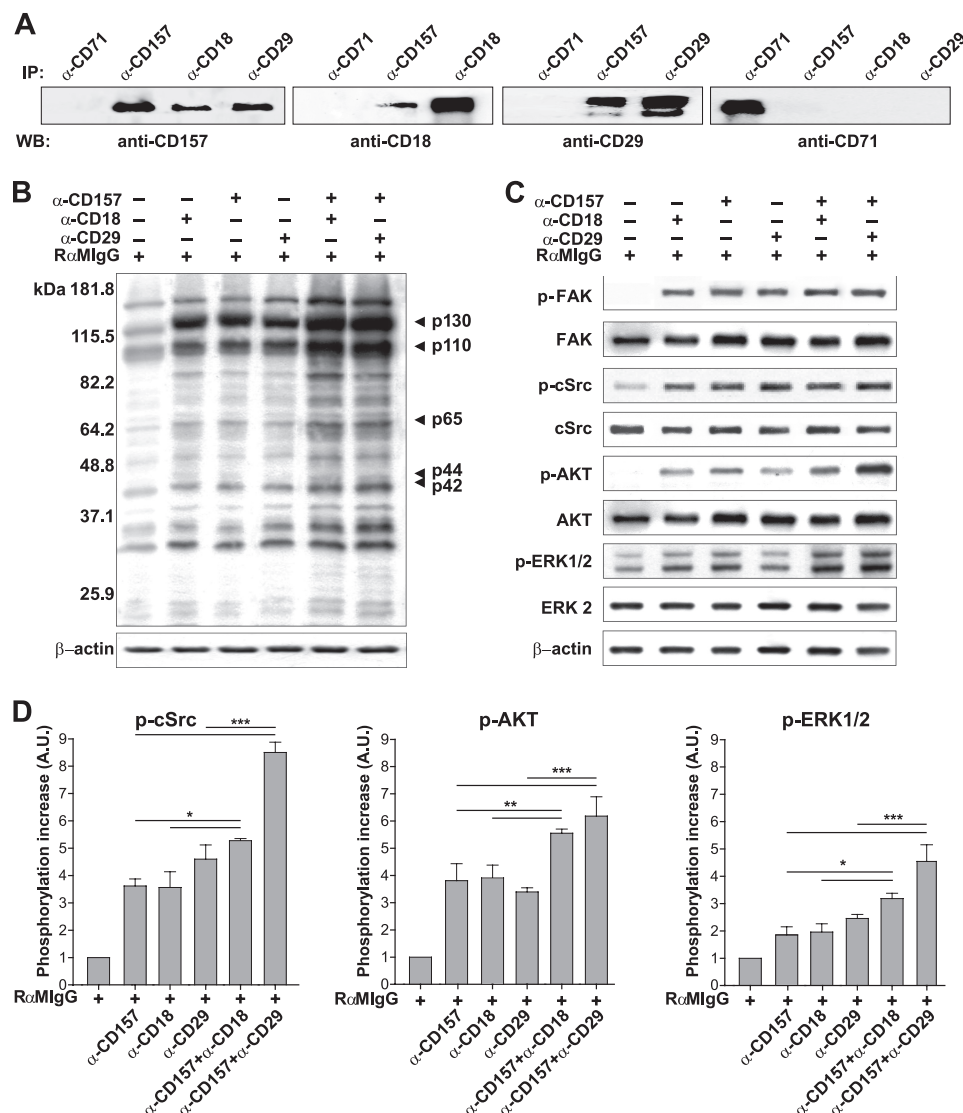
FIGURE 5. **CD157 interacts with integrins and induces intracellular signal transduction after cross-linking.** *A*, THP-1 cells lysates were immunoprecipitated (*IP*) with the indicated mAbs. Proteins were eluted, resolved on 10% SDS-PAGE, and analyzed by Western blotting (*WB*) using anti-CD157, anti-CD18, anti-CD29, or anti-CD71 mAbs. Western blotting was performed three times, and a representative example is presented. *B*, THP-1 cells were incubated with F(ab')$_2$ anti-CD157, CD18, and CD29 mAb (5 μg/ml) followed by F(ab')$_2$ RαMIgG (20 μg/ml for 10 min at 4 °C and 1 min at 37 °C) and lysed. To induce combined engagement of CD157 and CD18 or CD157 and CD29 on plasma membrane, THP-1 cells were simultaneously incubated with the indicated primary mAbs (10 min at 4 °C) followed by F(ab')$_2$ RαMIgG. Total lysates (30 μg/lane) were resolved on 10% SDS-PAGE, immunoblotted, and probed with HRP-labeled anti-phosphotyrosine antibody. *C*, THP-1 cells were incubated with the indicated primary mAb followed by F(ab')$_2$ RαMIgG. Immunoblots were probed with anti-phospho-FAK (*p-FAK*), anti-phospho-c-Src (*p-cSrc*), anti-phospho-AKT (*p-AKT*), or anti-phospho-ERK1/2 antibody (*p-ERK1/2*). β-Actin was used as loading control. The membranes were stripped and reprobed with anti-FAK, anti-c-Src, anti-AKT, and anti-ERK2 antibodies detecting the total form of each protein followed by incubation with the appropriate HRP-conjugated antibodies. One representative experiment of three is shown. *D*, the increased phosphorylation of c-Src (*left*), Akt (*middle*), and ERK2 (*right*) induced by CD157 cross-linking on THP-1 cells was quantified and compared with that induced by combined cross-linking of either CD157 plus CD18 or CD157 plus CD29. Images were scanned using an image scanner and quantitatively analyzed using the software package NIH ImageJ 1.43 (National Institutes of Health, Bethesda, MD). Results are means ± S.E. of three separate experiments and are expressed as -fold increase in phosphorylation as compared with that obtained by treating cells with the F(ab')$_2$ RαMIgG alone (20 μg/ml, basal phosphorylation = 1). *, $p < 0.05$, **, $p < 0.01$, and ***, $p < 0.001$. *A.U.*, arbitrary units.

CD157 is a GPI-anchored molecule with no intrinsic signaling capacity; it has been hypothesized that the molecule establishes physical association with transmembrane receptors to transduce signals. The structural association between CD157 and both β_1 and β_2 integrin and the coexistence of CD157 with selected integrins in specific membrane domains provided the rationale for identifying integrins as likely candidates for being CD157 partner proteins. Evidence was sought by inducing combined clustering of CD157 and β_1 integrin or CD157 and β_2 integrin on the plasma membrane of THP-1 cells by means of

antibody cross-linking. The results showed that concurrent ligation of CD157 with either CD18 or CD29 is accompanied by a sharp increase in phosphorylation of c-Src, Akt, and ERK1/2, with no variations in the absolute amount of c-Src, Akt, and ERK1/2 in the cell lysates (Fig. 5, *B–D*). These results indicated that CD157 can use both β_1 and β_2 integrins as tools in signal transduction. This leads to the activation of distinct downstream signaling pathways converging on the MEK/ERK pathway, which is responsible for controlling crucial aspects of monocyte extravasation.

DISCUSSION

Monocyte recruitment to extravascular sites is an important component of the inflammatory response to a variety of stimuli such as bacterial infections, tumor growth, and atherosclerotic plaque formation. The surface expression and release (as soluble proteins or membrane vesicles) (34) of a number of molecules serves to coordinate and fine-tune the local inflammatory response according to the particular circumstances. Here we present evidence that CD157 is one of these molecules. We used antibody-mediated cross-linking of CD157 to mimic its natural clustering (a strategy commonly adopted for initiating signal transduction, although the actual mechanism of how this works remains unclear) and demonstrated that CD157 cross-linking promotes β_1 and β_2 integrin relocation and orchestrates the assembly of signaling-competent membrane domains. The outcome is regulation of monocyte behavior. This unique role of CD157 accounts for its involvement in critical functions of monocytes, including (i) transendothelial migration and (ii) adhesion to ECM proteins. CD157 operates both in non-inflammatory as well as in inflammatory conditions. Indeed, the extent of the inhibitory effects of blocking mAb on transmigration across quiescent and activated endothelium is comparable. However, forced clustering of CD157 through the addition of a secondary cross-linking antibody at the beginning of or during the process is sufficient to significantly restore transmigration, suggesting that CD157 cross-linking triggers signal transduction. The results obtained in adhesion assays strengthened this assumption. Indeed, clustering of CD157 by the addition of a secondary cross-linking antibody to mouse IgG was able to revert the blockade induced by the anti-CD157 mAb. The originally described enzymatic functions of CD157 and CD38 (the other member of the NAD glycohydrolase/ADP-ribosyl cyclase gene family) have progressively given way to a burgeoning array of functions in activation signaling (35, 36) and lateral associations with multiple partner molecules on the plasma membrane (36–38).

We demonstrated that antibody-induced CD157 aggregation can elicit rapid intracellular Ca^{2+} mobilization and promote neutrophil polarization. The efficiency of these effects is proportional to the extent of cross-linking, suggesting that the aggregation of many molecules is crucial to the formation of competent signaling microdomains (11). In alignment with this observation, here we demonstrated that anti-CD157 mAb, which can cross-link two molecules, is not sufficient to drag integrins into rafts and, consequently, to transduce activation signals; hence, it blocks transmigration and adhesion, likely preventing leukocyte interaction with a so far unidentified physiological ligand(s). Further work will be required to unravel the actual molecular mechanism by which the antibody blockade of CD157 interferes with monocyte transmigration and adhesion to ECM proteins.

CD157 is bound to the cell membrane by a GPI anchor. This means that it has no access to the cytoplasmic face of the plasma membrane and therefore lacks direct contact with intracellular signaling intermediates. Although the mechanisms underlying signal transduction through GPI-anchored proteins are not fully understood, an accepted model is that these molecules create complexes with membrane-spanning proteins, which then act as a signal transduction device. Here we demonstrated that in human monocytes, CD157 forms a multimolecular complex with integrins. Indeed, according to the co-immuno-precipitation experiments, it is physically bound to CD18 and CD29; furthermore, it functionally interacts with both integrins, as highlighted by adhesion assays.

GPI-anchored proteins are generally concentrated in lipid rafts, which are microdomains within the plasma membrane enriched with glycosphingolipids, cholesterol, and several signaling elements (39). Lipid rafts are thought to provide the milieu necessary for bringing discrete receptors and downstream intermediates into close proximity, thereby allowing the formation of signaling-competent microdomains. Our data showed that (i) CD157 is virtually entirely located within the lipid rafts on the THP-1 cell membrane and (ii) CD157 clustering causes CD18 and CD29 integrins to accumulate in the lipid rafts, much in the same way as with selected ECM proteins (40).

Activated β_1 and β_2 integrins, but not inactive molecules, were reported as preferentially localized in lipid rafts in lymphocytes (41). The recruitment of integrins into lipid rafts was postulated as being a mechanism regulating their activity (42). The affinity for lipid rafts is an inherent feature of integrins as it is shared by integrins activated in several ways (43). Conceivably, in addition to the interaction with their ligand, integrins could be held within the lipid rafts as a result of their lateral association with membrane proteins residing within them (44, 45). Our results demonstrate that this is the case for CD157 on monocytes. Indeed, following CD157 aggregation, a considerable amount of both CD18 and CD29 moves to the lipid raft compartment of the cell membrane, resulting in subsequent activation of downstream signaling. The ability to form large raft patches with signaling activity following cross-linking is a feature shared by GPI-anchored molecules (46); instead, the promotion of integrin compartmentalization into lipid rafts is not a prerogative of all GPI-anchored molecules. For example, CD87 cross-linking on myeloid cells is unable to promote β_2 integrin redistribution into lipid rafts (47). The existence of physical interactions between CD157 and integrins provides a compelling basis for motivating their functional interplay; however, the molecular bases supporting the structural interaction of CD157 with different integrins remain unclear and deserve further investigation. These findings indicate that CD157 (i) behaves as a molecular organizer of membrane microdomains and (ii) is part of the integrin-driven molecular machinery that regulates crucial functions of monocytes, including transendothelial migration and adhesion to ECM proteins.

To explore the signal transduction cascade raised by CD157 engagement, we assessed the phosphorylation status of selected proteins upon CD157 antibody cross-linking and demonstrated that CD157-mediated intracellular signaling relies on integrin/Src/FAK, leading to increased activity of downstream MAPK/ERK1/2 and PI3K/Akt pathways. These pathways are core components of the integrin-mediated signaling network coordinating complex biological responses of monocytes, such as cell growth, adhesion, and migration, in normal and pathological conditions (48).

Role of CD157 in the Control of Monocyte Functions

In this dynamic interplay between CD157 and integrins, not only does CD157 share effector targets with β_1 and β_2 integrins, which represent crucial checkpoints of leukocyte trafficking, but it also acts as a stimulatory molecule and cooperates with both integrins in the control of cell migration and adhesion. Indeed, concurrent engagement of CD157 and integrins resulted in increased tyrosine kinase receptor phosphorylation and PI3K and MAPK signaling cascade activation. This is consistent with previous reports demonstrating the need to aggregate integrins on monocyte plasma membrane to achieve maximal tyrosine phosphorylation leading to optimal effector functions (49, 50).

It is easy to imagine that in a physiological context, CD157 engagement by its non-substrate ligand (so far unknown) recruits pre-existing β_1 and β_2 integrin nanoclusters (50) into lipid rafts, thus influencing their three-dimensional organization and promoting the transduction of intracellular signals, which drive efficient cytoskeletal rearrangements, cell adhesion, and transmigration. These conclusions are further supported by the observation that neutrophils from patients with paroxysmal nocturnal hemoglobinuria (which express neither CD157 nor other GPI-anchored molecules as a result of an acquired genetic mutation) (51) are characterized by defective transendothelial migration and adhesion to ECM proteins (11, 14).

It is tempting to speculate that the spatial reorganization induced *in vitro* by mAb cross-linking is a general mechanism implemented *in vivo* by the interaction between CD157 and its ligand to offer cells (leukocytes or ovarian tumor cells (9)) with privileged areas for optimal response to the outside environment. The identification of a non-substrate ligand of CD157 is expected to shed light on these issues.[6]

In conclusion, these results begin to outline a model where CD157 controls leukocyte extravasation through relocation of integrins into signaling-competent microdomains (*i.e.* signalosomes), which are required to efficiently recruit protein tyrosine kinases and scaffolding proteins and to switch on the complex network of interconnected signaling pathways (21, 52).

Integrins are attractive targets for the treatment of inflammatory and autoimmune diseases, and several specific antibodies have been tested in clinical trials. However, the integrin-blocking approaches have significant side effects related to impaired host response (53). The existence of CD157 as an integrin-associated molecule that mediates specific functions offers the potential for fine-tuning integrin functions and permitting the development of improved therapeutic strategies in inflammatory diseases such as arthritis and atherosclerosis.

REFERENCES

1. Salmi, M., and Jalkanen, S. (2005) *Nat. Rev. Immunol.* **5,** 760–771
2. Airas, L., Niemelä, J., and Jalkanen, S. (2000) *J. Immunol.* **165,** 5411–5417

3. Mina-Osorio, P., Winnicka, B., O'Conor, C., Grant, C. L., Vogel, L. K., Rodriguez-Pinto, D., Holmes, K. V., Ortega, E., and Shapiro, L. H. (2008) *J. Leukoc. Biol.* **84,** 448–459
4. Ossowski, L., and Aguirre-Ghiso, J. A. (2000) *Curr. Opin. Cell Biol.* **12,** 613–620
5. Frasca, L., Fedele, G., Deaglio, S., Capuano, C., Palazzo, R., Vaisitti, T., Malavasi, F., and Ausiello, C. M. (2006) *Blood* **107,** 2392–2399
6. Ferrero, E., and Malavasi, F. (1999) *J. Leukoc. Biol.* **65,** 151–161
7. Malavasi, F., Deaglio, S., Funaro, A., Ferrero, E., Horenstein, A. L., Ortolan, E., Vaisitti, T., and Aydin, S. (2008) *Physiol. Rev.* **88,** 841–886
8. Ortolan, E., Vacca, P., Capobianco, A., Armando, E., Crivellin, F., Horenstein, A., and Malavasi, F. (2002) *Cell Biochem. Funct.* **20,** 309–322
9. Ortolan, E., Arisio, R., Morone, S., Bovino, P., Lo-Buono, N., Nacci, G., Parrotta, R., Katsaros, D., Rapa, I., Migliaretti, G., Ferrero, E., Volante, M., and Funaro, A. (2010) *J. Natl. Cancer Inst.* **102,** 1160–1177
10. Ishihara, K., and Hirano, T. (2000) *Chem. Immunol.* **75,** 235–255
11. Funaro, A., Ortolan, E., Ferranti, B., Gargiulo, L., Notaro, R., Luzzatto, L., and Malavasi, F. (2004) *Blood* **104,** 4269–4278
12. Lavagno, L., Ferrero, E., Ortolan, E., Malavasi, F., and Funaro, A. (2007) *J. Biol. Regul. Homeost. Agents* **21,** 5–11
13. Todd, R. F., 3rd, and Petty, H. R. (1997) *J. Lab. Clin. Med.* **129,** 492–498
14. Ortolan, E., Tibaldi, E. V., Ferranti, B., Lavagno, L., Garbarino, G., Notaro, R., Luzzatto, L., Malavasi, F., and Funaro, A. (2006) *Blood* **108,** 4214–4222
15. Yona, S., and Jung, S. (2010) *Curr. Opin. Hematol.* **17,** 53–59
16. Ross, R. (1999) *N. Engl. J. Med.* **340,** 115–126
17. Kamei, M., and Carman, C. V. (2010) *Curr. Opin. Hematol.* **17,** 43–52
18. Springer, T. A. (1994) *Cell* **76,** 301–314
19. Luster, A. D., Alon, R., and von Andrian, U. H. (2005) *Nat. Immunol.* **6,** 1182–1190
20. Vestweber, D. (2007) *Immunol. Rev.* **218,** 178–196
21. Ley, K., Laudanna, C., Cybulsky, M. I., and Nourshargh, S. (2007) *Nat. Rev. Immunol.* **7,** 678–689
22. Shen, J., Ham, R. G., and Karmiol, S. (1995) *Microvasc. Res,* **50,** 360–372
23. Kusumi, A., and Suzuki, K. (2005) *Biochim. Biophys. Acta* **1746,** 234–251
24. Vonesch, C., and Unser, M. (2008) *IEEE Trans. Image Process* **17,** 539–549
25. Jaskolski, F., Mulle, C., and Manzoni, O. J. (2005) *J. Neurosci. Methods* **146,** 42–49
26. Jiang, Y., Beller, D. I., Frendl, G., and Graves, D. T. (1992) *J. Immunol.* **148,** 2423–2428
27. Liao, F., Huynh, H. K., Eiroa, A., Greene, T., Polizzi, E., and Muller, W. A. (1995) *J. Exp. Med.* **182,** 1337–1343
28. Randolph, G. J., and Furie, M. B. (1995) *J. Immunol.* **155,** 3610–3618
29. Florey, O., Durgan, J., and Muller, W. (2010) *J. Immunol.* **185,** 1878–1886
30. Korpos, E., Wu, C., and Sorokin, L. (2009) *Curr. Pharm. Des.* **15,** 1349–1357
31. Brown, D. A., and London, E. (2000) *J. Biol. Chem.* **275,** 17221–17224
32. Holleran, B. J., Barbar, E., Payet, M. D., and Dupuis, G. (2003) *J. Leukoc. Biol.* **73,** 243–252
33. Gaus, K., Le Lay, S., Balasubramanian, N., and Schwartz, M. A. (2006) *J. Cell Biol.* **174,** 725–734
34. Théry, C., Ostrowski, M., and Segura, E. (2009) *Nat. Rev. Immunol* **9,** 581–593
35. Liang, F., Qi, R. Z., and Chang, C. F. (2001) *FEBS Lett.* **506,** 207–210
36. Muñoz, P., Navarro, M. D., Pavón, E. J., Salmerón, J., Malavasi, F., Sancho, J., and Zubiaur, M. (2003) *J. Biol. Chem.* **278,** 50791–50802
37. Funaro, A., De Monte, L. B., Dianzani, U., Forni, M., and Malavasi, F. (1993) *Eur. J. Immunol.* **23,** 2407–2411
38. Deaglio, S., Zubiaur, M., Gregorini, A., Bottarel, F., Ausiello, C. M., Dianzani, U., Sancho, J., and Malavasi, F. (2002) *Blood* **99,** 2490–2498
39. Simons, K., and Toomre, D. (2000) *Nat. Rev. Mol. Cell Biol.* **1,** 31–39
40. Cherukuri, A., Dykstra, M., and Pierce, S. K. (2001) *Immunity* **14,** 657–660
41. Leitinger, B., and Hogg, N. (2002) *J. Cell Sci.* **115,** 963–972
42. Marwali, M. R., Rey-Ladino, J., Dreolini, L., Shaw, D., and Takei, F. (2003) *Blood* **102,** 215–222
43. van Zanten, T. S., Cambi, A., Koopman, M., Joosten, B., Figdor, C. G., and Garcia-Parajo, M. F. (2009) *Proc. Natl. Acad. Sci. U.S.A.* **106,** 18557–18562
44. Porter, J. C., and Hogg, N. (1998) *Trends Cell Biol.* **8,** 390–396
45. Streuli, C. H., and Akhtar, N. (2009) *Biochem. J.* **418,** 491–506

---

[6] A. Funaro, manuscript in preparation.

46. Harder, T., and Simons, K. (1999) *Eur. J. Immunol.* **29,** 556–562
47. Sitrin, R. G., Johnson, D. R., Pan, P. M., Harsh, D. M., Huang, J., Petty, H. R., and Blackwood, R. A. (2004) *Am. J. Respir. Cell Mol. Biol.* **30,** 233–241
48. Abram, C. L., and Lowell, C. A. (2009) *Annu. Rev. Immunol.* **27,** 339–362
49. Miyamoto, S., Akiyama, S. K., and Yamada, K. M. (1995) *Science* **267,** 883–885
50. Cambi, A., Joosten, B., Koopman, M., de Lange, F., Beeren, I., Torensma, R., Fransen, J. A., Garcia-Parajó, M., van Leeuwen, F. N., and Figdor, C. G. (2006) *Mol. Biol. Cell* **17,** 4270–4281
51. Luzzatto, L. (2006) *Curr. Opin. Genet. Dev.* **16,** 317–322
52. Rose, D. M., Alon, R., and Ginsberg, M. H. (2007) *Immunol. Rev.* **218,** 126–134
53. Clifford, D. B., De Luca, A., Simpson, D. M., Arendt, G., Giovannoni, G., and Nath, A. (2010) *Lancet Neurol.* **9,** 438–446